Title: Focused Ultrasound modulates dopamine in a mesolimbic reward circuit

Authors: Greatness O. Olaitan [a], Mallikarjunarao Ganesana [a], Wendy J. Lynch [b], Wynn Legon [c,d], B. Jill Venton [a*]

Institutions/Affiliations:

a. Department of Chemistry, University of Virginia, Charlottesville, VA, USA
b. Psychiatry and Neurobehavioral Sciences, University of Virginia, Charlottesville, VA, USA
c. Fralin Biomedical Research Institute at Virginia Tech Carilion, Roanoke, VA, USA
d. School of Neuroscience, Virginia Polytechnic Institute and State University, Blacksburg, VA, USA

Abstract:

Dopamine is a neurotransmitter that plays a significant role in reward and motivation. Dysfunction in the mesolimbic dopamine pathway has been linked to a variety of psychiatric disorders, including addiction. Low-intensity focused ultrasound (LIFU) has demonstrated effects on brain activity, but how LIFU affects dopamine neurotransmission is not known. Here, we applied three different intensities (6.5, 13, and 26 W/cm^2 Isppa) of 2-minute LIFU to the prelimbic region (PLC) and measured dopamine in the nucleus accumbens (NAc) core using fast-scan cyclic voltammetry. Two minutes of LIFU sonication at 13 W/cm^2 to the PLC significantly reduced dopamine release by ~ 50% for up to 2 hours. However, double the intensity (26 W/cm^2) resulted in less inhibition (~30%), and half the intensity (6.5 W/cm^2) did not result in any inhibition of dopamine. Anatomical controls applying LIFU to the primary somatosensory cortex did not change NAc core dopamine, and applying LIFU to the PLC did not affect dopamine release in the caudate or NAc shell. Histological evaluations showed no evidence of cell damage or death. Modeling of temperature rise demonstrates a maximum temperature change of 0.5°C with 13 W/cm^2, suggesting that modulation is not due to thermal mechanisms. These studies show that LIFU at a moderate intensity provides a noninvasive, high spatial resolution means to modulate specific mesolimbic circuits that could be used in future studies to target and repair pathways that are dysfunctional in addiction and other psychiatric diseases.

1. Introduction

Dopamine is a neuromodulator with many essential roles in the central nervous system.[1,2] In the mesolimbic system, dopaminergic neurons from the ventral tegmental area (VTA) innervate various brain regions, including the prefrontal cortex (PFC) and nucleus accumbens (NAc), and play a pivotal role in regulating feelings of well-being and reward. [3–6] A particularly notable circuitry within the reward pathway is the connection between glutamatergic neurons from the prelimbic region (PLC) of the medial PFC (mPFC) and dopaminergic neurons in the NAc core.[7–9] This circuitry regulates motivational aspects related to reward by controlling dopamine release in the NAc core. Dysregulation of this specific circuit is observed in reward-related diseases such as addiction and pathological gambling.[10] Consequently, re-regulating this glutamate-dopamine circuitry could provide a strategic approach to treating neuropsychological diseases involving the mesolimbic dopamine system.

Targeted neuromodulation represents a new frontier in the treatment of neuropsychological diseases, offering precise control over specific neural circuits that traditional pharmacological approaches fail to provide.[11–13] This specificity is crucial, especially in conditions associated with disruptions in dopamine, considering the diverse roles it plays in reward processing, motor control, and emotional responses.[14] Noninvasive methods to regulate neural activity, such as transcranial magnetic stimulation (TMS) and transcranial electrical stimulation (TES), have emerged as promising alternatives.[15,16] Although TMS and TES can exert both excitatory and inhibitory effects on neurotransmission, with some clinical successes, they are limited by poor spatial resolution and an inherent depth-focality tradeoff.[17] This limitation constrains their ability to target deeper brain areas with precision. In contrast, Low-Intensity Focused Ultrasound (LIFU) utilizes acoustic waves to modulate neuronal activity by focusing these waves on small, specific regions deep within the brain, as demonstrated in various animal models and human studies.[18,19] The capability of LIFU to precisely target circuits, such as the PLC

to NAc core circuit, presents a significant advancement in neuromodulation, offering insights into both normal and pathological brain states.

LIFU's potential to influence neurotransmitters, especially in the context of circuit-based neuromodulation, has been substantiated in animal models. For example, Xu et al. (2020) found that LIFU targeting the striatum in a Parkinsonian mouse model enhanced dopamine content as measured in this same brain region using High-Performance Liquid Chromatography (HPLC).[20] Similarly, Min et al. (2011) used microdialysis to demonstrate that LIFU targeting the thalamus significantly increased dopamine concentrations as assessed in its projection region to the striatum.[21] While encouraging, these studies are not able to capture rapid, real-time fluctuations in neurotransmitter release. Our study bridges this gap by employing fast-scan cyclic voltammetry, a technique that allows for the real-time measurement of neurotransmitter dynamics, to understand the time course of LIFU to inhibit dopamine [22].

The goal of this study was to determine the effect of LIFU to the PLC on real-time changes in dopamine release in its projection region to the NAc core. We explored three different LIFU intensities (6.5 W/cm^2, 13 W/cm^2, and 26 W/cm^2 I_{sppa}) to determine the conditions most effective in inhibiting dopamine release, as measured using fast-scan cyclic voltammetry (FSCV).[23,24] We also measured dopamine release in adjacent regions of the striatum (NAc shell, caudate) in order to establish circuit specificity and determined effects on NAc core dopamine release following LIFU modulation of adjacent cortical and sub-cortical regions (i.e., caudate and somatosensory cortex). We hypothesized that higher LIFU intensities applied to the PLC would result in greater suppression of dopamine release within the connected NAc core circuit. We further hypothesized that effects on dopamine release would be specific to LIFU targeting the PLC, with observable changes in the NAc core but not in the NAc shell. Given the role of the PFC-NAc dopaminergic circuit in reward-related neuropsychiatric disorders, elucidating the intensity-dependent and

circuit-specific effects of LIFU on dopamine inhibition holds promise for diverse therapeutic applications.

Results

Ultrasound Characterization

Fig. 1A shows a pseudo color axial (Z) pressure map overlaid to scale on a rat brain atlas to show overlap with the desired sonicated area (PLC). The lateral XY and XZ pressure maps are shown in Figure 1B and Figure 1C. The full-width half maximum (FWHM) in the XY plane was ~ 0.7 mm, while the FWHM in the Z axis was 6 mm.

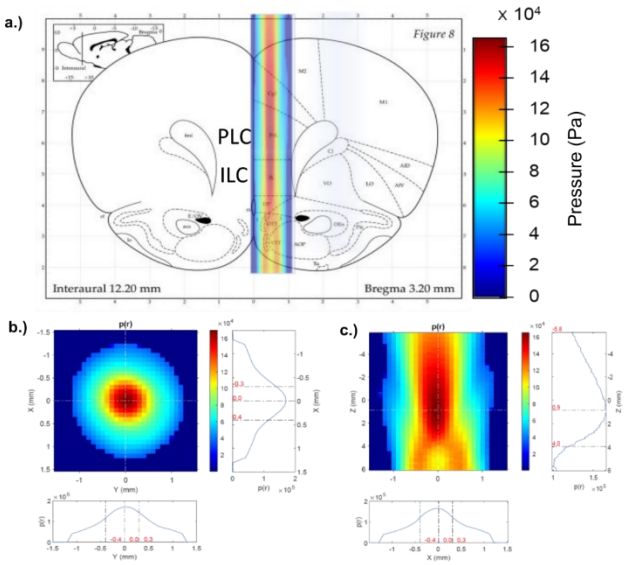

Figure 1: Characteristics of Low-Intensity Focused Ultrasound Sonication. (a). Overlay of coronal rat brain section and LIFU acoustic waves z-plane showing highest LIFU intensity at pre-limbic region. **(b.)** x-y planes of LIFU acoustic waves showing peak intensity focused within a ~0.7 mm diameter. Vertical dashed lines on line plots show a -3dB range. **(c.)** x- z planes of LIFU acoustic waves showing peak intensity focused at ~6-7 mm from the exit plane of the transducer (bottom pointing up). Vertical dashed lines on line plots denote the -3dB range.

Ultrasound Heating Modelling

Models were run using the three different intensities. **Figure 2** shows the predicted temperature rise over the 2-minute sonication. The starting temperature was set at 37°C. The maximum predicted temperature rise for 6.5 W/cm^2 was 37.2°C, 13 W/cm^2 was to 37.4°C, and 26 W/cm^2 to 37.9°C. These temperature rises would not constitute a thermal mechanism and are less than the natural brain fluctuation.[25]

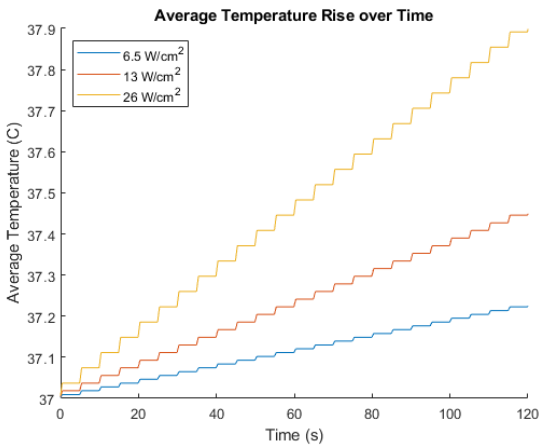

Figure 2: Modeling of ultrasound temperature rise. The figure shows estimated heating in the brain for the three tested intensities for the 2 minutes of sonication.

Stimulated Dopamine Control

To ensure that stimulated dopamine release was stable for the length of our experiments, we collected data without LIFU for two hours and thirty minutes in 4 animals. Figure 3A shows the experimental setup for the no-LIFU control experiments where the carbon-fiber recording electrode is placed at the NAc core, and the stimulating electrode is placed at the VTA. Figure 3B shows typical stimulated dopamine release with a color plot, concentration vs. time trace, and cyclic voltammogram.[24] Dopamine rises when stimulated and decreases again to baseline in a few seconds. The color plot and voltammogram identify the species detected as dopamine.[23] Dopamine release was stable over the first hour and slightly decreased after that, decreasing to 83 ± 2% compared to the first 30 minutes baseline (Fig. 3C); however, the decrease was not statistically significant (One-Way ANOVA, $p = 0.0615$, $F_{(2, 6)} = 4.598$, $n = 4$) (Figure 3D). Following

the calibration of the electrodes after the experiment, an average dopamine release of 200 ± 9 nM (range: 170 nM – 313 nM) was observed.

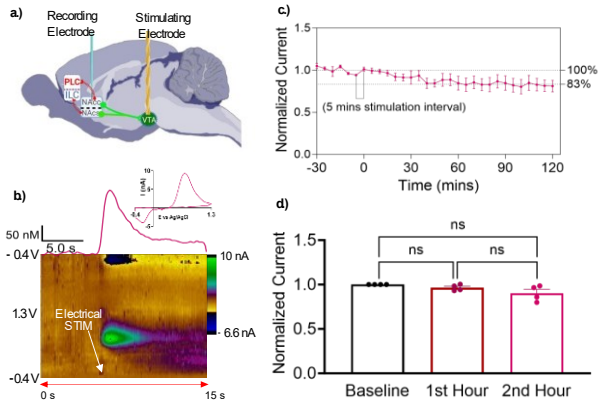

Figure 3: Stimulated Dopamine Control. a) Experimental setup: For the no-LIFU control experiments, the carbon-fiber recording electrode was placed at the NAc core, and the stimulating electrode was placed at the VTA. **b) (Top)** Concentration vs. time curve. The color plot and voltammogram show 200 ± 4 nM dopamine release at the carbon-fiber microelectrode (recording electrode) surface using FSCV. **c)** Group (n = 4) mean ± SEM dopamine release over time was measured every 5 minutes. After 2 hours, dopamine release reduction was 17 ± 0.3 %. **d)** Group (n = 4), mean ± SEM, data from C grouped into baseline and 1-hour blocks. Dopamine release did not significantly change in the first hour and second hour post-LIFU sonication as compared to baseline p = 0.21.

PLC LIFU Sonication Causes Dopamine Release Inhibition in the NAc Core.

Next, we tested the effects of inhibitory LIFU in the mesolimbic circuit. We hypothesized that applying LIFU to the PLC would inhibit dopamine release in the NAc core (Fig. 4A) since PLC glutamatergic projections regulate NAc core dopamine.[26] Fig. 4B shows the dopamine data with 13 W/cm^2 intensity, including the color plot concentration vs. time curves (Figure 4B). The color plot shows the dopamine release is lower (less green color intensity), and the concentration vs. time curves show the peak current decreased from 7 nA to 3.5 nA. The dopamine concentration dropped from 160 ± 10 nM to 82 ± 5 nM, a 50 ± 3 % decrease. Figure 4C shows the averaged data for n=7 rats, and inhibition was observed 2 minutes after sonication with 13 W/cm^2 LIFU, and dopamine release continued to be inhibited for 2 hours after a single LIFU treatment. Fig. 4D shows that LIFU sonication of the PLC evoked a 42 ± 3 % dopamine inhibition in the first hour and an additional 7 ± 1 % in the second-hour post-LIFU sonication. There is a significant effect

of LIFU on dopamine release in the first hour versus Pre-LIFU (One-way ANOVA, $p < 0.0001$, $F_{(2, 12)} = 66.4$, n=7) as well as the second hour ($p<0.0001$), but there was no difference between the 1-hour and 2-hour data ($p = 0.2668$).

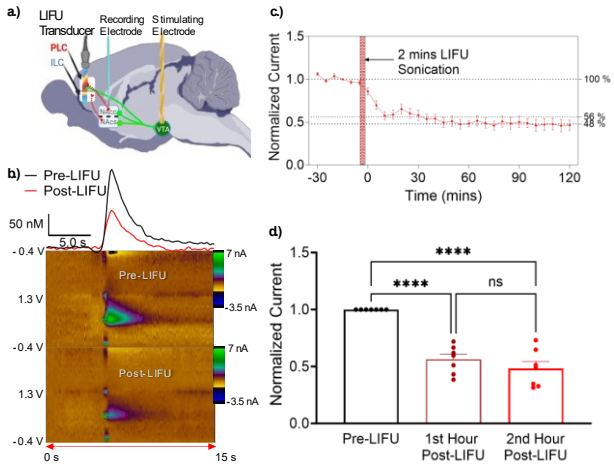

Figure 4: Prelimbic Region LIFU Inhibited Dopamine Release in the Nucleus Accumbens. a) The LIFU transducer was placed above the brain for the PLC sonication. **b)** Color plots and concentration-time trace show the inhibition of dopamine release from 160 ± 10 nM to 82 ± 5 nM after 2 hours post-LIFU. **c)** Group (n = 7) mean ± SEM. Normalized current over time**.** The vertical red bar denotes the application of 2 minutes of LIFU to PLC. Dopamine release was tested every 5 minutes out to 2 hours after LIFU. **d)** Group (n = 7) mean ± SEM. Data from C collapsed into baseline and 1-hour bins. Focused ultrasound sonication of the PLC invoked a 42 ± 3 % average dopamine inhibition in the first-hour post-LIFU sonication that did not significantly change (7 ± 1 % ($p = 0.4356$)) in the second hour.

Effect of LIFU Intensity Dosing on Dopamine Inhibition

To investigate the effect of LIFU intensity on dopamine release, we halved (6.5 W/cm^2) and doubled (26 W/cm^2) the LIFU intensity while leaving all other parameters constant. Figure 5A shows the overlay of the concentration vs. time traces for dopamine release before and after LIFU sonication for both spatial peak average intensities. The dopamine release levels dropped from 180 ± 7 nM to 144 ± 5 nM with 6.5 W/cm$^{2.}$ and from 150 ± 5 nM to 100 ± 3 nM with 26 W/cm^2 (Figure 5A). Fig. 5B shows that, unlike the immediate drop in stimulated dopamine release with 13 W/cm^2, 6.5 W/cm^2, I_{SSPA} resulted in only about 20 ± 1% reduction in dopamine release, similar to the no-LIFU controls. Applying 26 W/cm^2 I_{SSPA} resulted in a 30 ± 1% gradual inhibition, taking

about 45 minutes (Figure 5B). In Figure 5C, sonicating the PLC with 13 W/cm^2 I_{SSPA} had the highest inhibitory effect on dopamine release in the NAc core (Mixed-effects analysis, $F_{(3, 18)} = 4.76$; $p < 0.0001$ and $n = 7$). 6.5 W/cm^2 I_{SSPA} showed no significant dopamine release inhibition 2 hours post-sonication (Mixed-effects analysis, $F_{(3, 18)} = 4.76$; $p = 0.2006$ and $n = 7$).

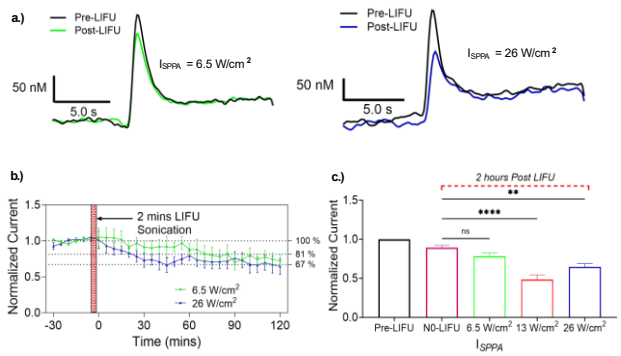

Figure 5: Intensity-Dependent Effects of LIFU on Dopamine Release in the Nucleus Accumbens. a) Concentration vs. time traces overlay and time-concentration scale bar show the change of dopamine release upon LIFU sonication. Sonication of PLC with 26 W/cm^2 I_{SPPA} reduced the dopamine release from 150 ± 5 nM to 100 ± 3 nM. The average dopamine release reduced from 180 ± 7 nM to 144 ± 5 nM with 6.5 W/cm^2 **b)** As a confirmation of the overlayed I-t curves, the 2-hour-long dopamine stimulation shows a 30 ± 1.0% change with 26 W/cm^2 I_{SPPA} and a 20 ± 0.7 % change with 6.5 W/cm^2 $I_{SPPA,}$ both with a 5-minute stimulation interval. **c)** Bar graph of a summarized result of dopamine changes with the tested LIFU parameters—in the order of dopamine inhibition, 13 W/cm^2 I_{SPPA} > 26 W/cm^2 I_{SPPA} > 6.5 W/cm^2 I_{SPPA}.

Circuit Specificity for the Inhibitory Effects of LIFU

To ensure that LIFU precisely inhibits the dmPFC circuit, specifically as opposed to the potential for non-specific effects,[27] we conducted three anatomical control experiments: (1) leaving the working electrode in the NAc core but applying LIFU to the primary somatosensory cortex (S1J-NAc core), (2) moving the working electrode to the caudate-putamen but leaving the LIFU in the PLC (PLC-CP) and (3) moving the working electrode to the NAc shell but leaving the LIFU in the PLC (PLC-NAc shell). In all cases, the brain was sonicated with 13 W/cm^2 I_{SSPA} since it gave the highest inhibition of dopamine among the tested intensities. Since S1J does not directly regulate NAc core dopamine release,[28] and the PLC does not regulate dopamine release in the CP or NAc shell,[29] we expected no significant inhibition of dopamine release in all cases. As

expected, dopamine release did not notably decrease in the S1J-NAc core, as it decreased from 150 ± 45 nM to 127.5 ± 4 nM, which is similar to controls (Fig. 6A). For the PLC-CP and the PLC-NAc shell control, dopamine release decreased from 160 ± 3 nM to 138 ± 3 nM and 118 ± 4 nM to 101 ± 3 nM, respectively, also similar to controls (Fig. 6A). On average, dopamine levels reduced gradually by 25 ± 1 % in the S1J-NAc core control, 14 ± 1 % in the PLC-CP control and 19 ± 1 % in the PLC-NAc shell control in 2 hours post-sonication (Figure 6B). Figure 6C shows that there is no significant difference between the dopamine level reduction with the No LIFU stimulated dopamine control and each anatomical control (Mixed-effects analysis, $F_{(2, 7)} = 4.76$; $p = 0.8561$ and $n = 4$ for S1J – NAc core, >0.9999 and $n = 4$ for PLC – CP; $p = 0.9700$ and $n = 4$ for PLC – NAc shell).

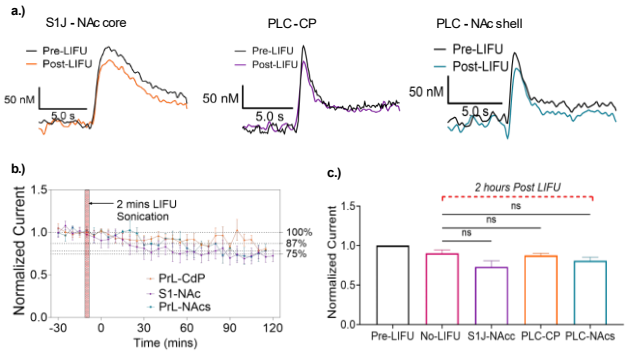

Figure 6: Circuit-Specificity of LIFU Neuromodulation. a) Concentration vs. time traces for anatomical controls for LIFU sonication with 13 W/cm^2 I_{SPPA}. Top: S1J-NAc core control showed a dopamine concentration change of 150 ± 5 nM to 128± 4 nM. Middle: PLC-CP control showed a concentration change of 160 ± 3 nM to 138 ± 3 nM. Right: PLC-NAc shell control showed a concentration change of 118 ± 4 nM to 101 ± 3 nM **b)** Dopamine stimulation data shows a 25 ± 0.8 % change in the S1J-NAc core control, a 14 ± 1 % change in the PLC-CP control, and a 19 ± 1 % change in the PLC-NAc shell control with 13 W/cm^2 I_{SPPA} after 2 hours. **c)** Bar graph of a summarized result of dopamine release change in the anatomical controls compared to the No-LIFU control after 2 hours post-LIFU. There was no significant difference between the initial dopamine release and the last dopamine release after the 2 hours of LIFU sonication.

No Effect of LIFU on Markers of Cell Damage or Death

Figure 7 shows standard bright field images of Hematoxylin and Eosin (H&E) -stained coronal sections of the PLC. As shown by the intactness of most nuclei (purple), no significant cell damage was observed with the No-LIFU Control (Figure 7A), 6.5 W/cm^2 LIFU I_{SSPA} (Figure 7B), 13 W/cm^2

LIFU I_{SSPA} (Figure 7c), or 26 W/cm^2 LIFU I_{SSPA} (Figure 7D). The bar graph in Figure 7E inset compares the nuclei count of the right brain PLC (LIFU-sonicated) to the left brain PLC of each animal (control). Mixed-effects analysis in Figure 7E shows no significant difference between the cell count of the treated (right) and untreated hemispheres (left) of any groups ($F_{(4,3)} = 4.76$, p=0.9412, n=4 for No-LIFU control, p=0. 9893 for 6.5 W/cm^2 I_{SPPA}, n=4, p>0.9999 for 13 W/cm^2 I_{SPPA}, n=4 and p=0.2557 for 26 W/cm^2 I_{SPPA}, n=4). Figure 7F compares all the nuclei counts between the nuclei counts of the sonicated PLC versus the No-LIFU controls. There was no significant difference in the nuclei counts of the sonicated PLC 1-hour post-test compared to control (One-Way ANOVA; $F_{(1.5, 4.6)} = 3.945$, p = 0.3959 for 6.5 W/cm^2 I_{SPPA}, p = 0.1701 for 13 W/cm^2 I_{SPPA}, and p = 0.6366 for 26 W/cm^2 I_{SPPA}).

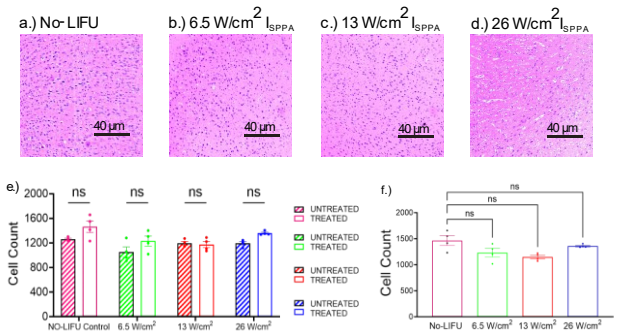

Figure 7. LIFU does not result in cell damage or death. Comparison of LIFU sonicated right pre-limbic area with non-sonicated left pre-limbic area. **a)** No-LIFU Control. **b)** 6.5 W/cm^2 LIFU I_{SSPA}. **c)** 13 W/cm^2 LIFU I_{SSPA}. **d)** 26 W/cm^2 LIFU I_{SSPA}. **e)** The bar graph shows no significant change in the treated (right) brain pre-limbic region LIFU sonicated nuclei count versus the left (untreated) brain control pre-limbic region. **f)** The bar graph shows no significant change between the nuclei counts of the right brain pre-limbic region of the sonicated brains versus the No-LIFU controls.

3. Discussion

The purpose of this study was to determine the use of LIFU as a tool for inducing circuit-specific inhibitory neuromodulation of dopamine. We investigated the impact of low-intensity focused ultrasound (LIFU) on real-time dopamine release within the PLC and its projection region, the NAc core. The primary finding was that a 2-minute LIFU treatment of the PLC with an I_{SSPA} of 13 W/cm^2

robustly (~50%) and persistently (2-hr) inhibited dopamine release in the NAc core. LIFU-induced inhibition was intensity-dependent, but not in a linear manner, as doubling the intensity to 26 W/cm^2 decreased the inhibition to 30%, and reducing intensity to 6.5 W/cm^2 did not significantly affect dopamine release as compared to controls. Effects were also circuit-specific. LIFU to the somatosensory cortex did not impact dopamine release in the NAc core, and LIFU to the PLC did not affect dopamine release in the caudate or NAc shell. LIFU did not result in appreciable heating and caused no cell damage or death, suggesting it can safely modulate the PLC, resulting in robust downstream neural circuit effects. These findings have strong translational implications, especially considering that ultrasound technology is already FDA-approved for human use. This study, therefore, positions LIFU as a noninvasive, precisely targeted, and effective tool for modulating dopaminergic neural circuits.

LIFU Sonication of PLC Results in a Downstream Dopamine Inhibition

This study demonstrates that phasic dopamine release in the NAc core is inhibited by sonicating the PLC. A 2-minute application of LIFU sonication to the PLC resulted in persistent suppression of electrically stimulated phasic dopamine release. Our experimental design in anesthetized animals did not allow a longer measurement of dopamine inhibition beyond two hours. However, future experiments could use a chronic electrode implantation design to determine how long the inhibition lasts.[30] Nonetheless, we show that inhibition lasts at least two hours, which demonstrates that even a brief LIFU treatment (2-min) leads to persistent neurochemical change.

Many studies have used the NAc core as a readout of activity in the dmPFC, and we used that same experimental design.[31–33] The reduction in dopamine level is proposed to be an effect of the inhibition of PLC-NAc core glutamatergic neurons. This hypothesis is based on previous studies showing that glutamatergic projections from the PLC to the NAc core function in a dopamine-dependent manner, where an increase in the neuronal activity of the PLC gives a

corresponding increase in the neuronal activity of the NAc core.[9,26,34,35] Our findings support the hypothesis that inhibitory LIFU parameters mediate the observed suppression of dopamine release in the NAc core. This effect potentially represents a downstream consequence of reduced glutamatergic activity from PLC neurons. While we cannot measure glutamate with FSCV because it is not electroactive, we measured the downstream effects on dopamine in the NAc core and saw inhibition.[36–38] Future studies could use a different technique, like genetically encoded sensors or biosensors, to measure glutamate[39]. Still, the downstream effects show that modulating the PLC with inhibitory LIFU results in downstream inhibition of dopamine release.

In the control group without LIFU, data indicated a modest 14-17% decrease in dopamine after 2 hours of VTA electrical stimulation, indicating fairly stable release without LIFU. It is noted in the literature that urethane anesthesia, which was used in our study, typically leads to a ~20% decrease in dopamine release due to its suppressive effects on striatal neuronal activity and basal dopamine concentrations.[40,41] In addition, previous research shows that prolonged electrical stimulation of the medial forebrain bundle slowly reduces presynaptic dopamine vesicular stores in the NAc.[42,43] Here, we employed short stimulation trains coupled with 5-minute recovery periods to mitigate the effects of prolonged stimulation. However, the reductions in dopamine signaling with LIFU are much larger than control, at ~ 30 % (26 W/cm^2) and ~ 49% (13 W/cm^2). Thus, inhibition is attributed to LIFU-induced inhibitory neuromodulation of the PLC-NAc core circuit rather than changes in dopamine cells from repeated stimulation alone.

While the focused ultrasound beam is centered in the PLC, about 40% of the maximal LIFU intensity may have targeted the infralimbic cortex (ILC). The ILC projects directly to the NAc shell and does not directly affect dopamine release in the core.[29] As a control, we applied LIFU to the PLC (which could result in 40% LIFU intensity reaching the ILC) and found that it did not affect stimulated dopamine release in the NAc shell. Thus, LIFU effects were restricted to the beam maximum, and the LIFU was applied in a sscircuit-specific manner.

Low-Intensity Focused Ultrasound Parameters for Dopamine Inhibition

Ultrasound influences physiological activity based on the parameters employed that may determine the mechanisms of action.[18] While this study was not specifically designed to investigate its mechanism of action, we were interested in the effect of intensity as this parameter may be a primary driver of LIFU neuromodulation. Typically, lower intensities are preferred as this poses a lower damage risk. Safety is an obvious concern in humans, particularly thermal effects. As such, we modeled the temperature rise using a simplified one-dimensional linear model using the Pennes bioheat equation, as has previously been performed in LIFU studies.[44] Darrow et al. (2019) showed that LIFU-induced temperature changes of 1 – 2 °C significantly suppressed somatosensory evoked potentials.[45] However, Yoo et al. (2011) showed that temperature changes of 0.7°C at 23 W/cm^2 did not contribute to neuromodulation.[46] The modeled temperature rises in this study were < 1°C after 2 minutes of ultrasound and only 0.4°C for the optimal dose, which falls below the proposed temperature change needed for neuromodulation. Thus, the LIFU mechanism in this study is likely non-thermal, and the parameters used are within safe limits for human ultrasound diagnostics.[47] The putative mechanisms of low-intensity focused ultrasound are largely believed to be mechanical due to the low frequency and low intensities employed.[48,49]

The impact of intensity on neurotransmitter release in this study does not follow a linear pattern, suggesting that increasing or decreasing the intensity can come at a cost in terms of LIFU effects on neurotransmitter release. Our data aligns with findings in humans that used the same PRF and duty cycle.[50,51] However, doubling the intensity did not result in increased inhibition, while halving the intensity led to only a minor inhibition following a quadratic function. Non-linear intensity effects have been previously observed. King et al. (2013) observed non-linear increases in evoked responses from EMG signals upon sonication intensities varied from 0-16.8 W/cm^2.[52] A lower inhibition level of dopamine by 26 W/cm^2 compared to 13 W/cm^2 is similar to the trend observed by Hoffman et al. (2022), where evoked action potential in mouse sensory neurons was

reduced between 11 and 30 W/cm^2 upon the activation of mechanically gated ion channel PIEZO2.[53] Ion channels do not always exhibit a linear response to neuronal firing, as their response is complex and contingent on several factors.[54] Consequently, the relationship between neurotransmitter release and neuronal firing, as well as ultrasound dose, may not be linear due to the intricate mechanism behind ion flux and the opening of neurotransmitter storage pools. Previous studies have demonstrated that LIFU directly activates mechanosensitive potassium channels, potentially leading to the termination of action potentials or causing calcium accumulation and ion channel amplification, thereby inducing neuronal excitation.[55–57] Mechanically gated channels may not open linearly with ultrasound application, and higher intensities may activate other channels. This study underscores the importance of directly measuring neurotransmitter release to understand the neuromodulation of LIFU, as effects may be non-linear. Further investigation is warranted to elucidate the precise mechanisms of LIFU-mediated neurotransmission.

This study demonstrates the inhibition of dopamine release by applying LIFU to a specific circuit in the rat brain. This basic research finding could be translational as LIFU is approved for use in humans. Yakuub et al., 2023 have previously shown that LIFU can modulate both neurochemical (GABA) and functional connectivity changes in the human anterior cingulate cortex.[58] Thus, the results we present in this study extend the knowledge of LIFU modulation of circuits to an important circuit in treating neuropsychological disorders involving the PLC and NAc. Recently, the use of ultrasound to treat substance use disorder in humans through the direct modulation of the NAc is being explored.[59] Mahoney et al., 2023 used both 55 and 80 W/cm^2 and a 3.3% duty cycle and 10-minute-long NAc sonication to reduce cue-induced substance craving activity – an indirect indication of local NAc dopamine inhibition.[59] With the shorter sonication duration and the circuit-specific dopamine inhibition in this study, as opposed to local inhibition, the parameters in this study could be translated to transcranial LIFU humans. Although the human

skull presents a formidable barrier to ultrasound stimuli, larger transducers with lower acoustic frequency can be used to accommodate human skull attenuation. During late withdrawal in substance use disorder patients, the PLC is overactive and may overstimulate dopamine and cause relapse.[60,61] The protocols we developed for circuit-specific inhibition of dopamine could be translated to the safe treatment of humans during late addiction withdrawal. Further, these results could be useful in the context of other disorders, such as chronic pain, given the involvement of the NAc and the dopamine system in chronic pain and the recent findings in humans for LIFU to reduce pain. [28,62,63]

This study demonstrates that LIFU application to the PLC induces downstream inhibition of dopamine by inhibiting the mesolimbic circuit. These are the first studies to measure dopamine release in real-time following LIFU treatment and show that different LIFU intensities produce different levels of dopamine inhibition. Importantly, this is a very specific neuromodulation, as stimulating nearby regions does not affect NAc core dopamine release, and stimulating the PLC does not affect dopamine in the NAc shell. Thus, LIFU is a tool to specifically inhibit dopamine release in the NAc through regulation by the PLC. Future studies could examine different LIFU parameters to examine if the circuit could be excited or use the inhibition to modulate dopamine when it is overexcited in some disease states, such as addiction.

Methods

Chemicals and Materials

Sodium chloride, sodium sulfate, calcium chloride, sodium phosphate monohydrate, and paraformaldehyde were purchased from Sigma-Aldrich (St. Louis, MO). Potassium chloride and magnesium chloride were purchased from Thermo Fisher Scientific (Waltham, WA). Dopamine hydrochloride was dissolved in 0.1 M $HClO_4$ to make a 10 mM stock solution. Phosphate buffered saline (PBS; (131.25 mM NaCl, 3.00 mM KCl, 10 mM NaH_2PO_4, 1.2 mM $MgCl_2$, 2.0 mM Na_2SO_4,

and 1.2 mM $CaCl_2$) was used at pH 7.4 to dilute the dopamine stock solution to 1.0 μM. De-ionized water (EMD Millipore, Billerica, MA) was used to prepare all aqueous solutions.

Construction of Carbon Fiber Microelectrodes

Carbon fiber microelectrodes were made by aspirating single 7 μm T-650 carbon fibers (Cytec, Woodland Park, NJ) into glass capillaries (A&M Systems, Inc., Carlsborg, WA) and pulled into two using a vertical PE-22 Electrode Puller (Narishige, Tokyo, Japan). Under a microscope, the extended fibers were manually trimmed to 150–200 μm from the glass seal using a scalpel. Before each use, electrode tips were soaked in 70% v/w isopropyl alcohol for 24 hours and backfilled with 1 M KCl.

Fast-scan cyclic voltammetry and electrochemical measurements

Cyclic voltammograms of dopamine were obtained using a Chem-Clamp potentiostat (Dagan Corp., Minneapolis, MN) coupled to a UNC breakout box (UNC Electronics Shop, Chapel Hill, NC) with a 1 MΩ head stage. HDCV software (UNC at Chapel Hill) was used for data acquisition and analysis. Ag/AgCl wires were used as the reference electrodes. A 3-KHz low-pass filter was used to measure dopamine with a waveform that scanned from −0.4 to 1.3 V and back at 400 V/s at 10 Hz. Carbon Fiber Micro Electrodes were post-calibrated with 1.0 μM dopamine in PBS following animal experiments.

Animal experiments

All animal experiments were performed as approved by the Animal Care and Use Committee (ACUC) of the University of Virginia. Seven rats were used for the parameter test experiments, while 4 rats each were used for the control experiments, making a total of 37 rats used for this study. Male Sprague Dawley rats (Charles River Laboratories, Wilmington, MA, USA) between 280 - 320 g were anesthetized with urethane (0.3 ml/l00 g, 5% saline solution., i.p.). The rectal and core body temperature was maintained at 32°C using an isothermal pad (Delta Phase Pad;

Braintree Scientific, Braintree, MA, USA). Hourly checks were made on respiration and depth of anesthesia. During surgery, a local anesthetic (bupivacaine) was used on exposed skin and muscle tissue.

The rat was placed in a stereotaxic frame, and holes were drilled precisely in the skull to place the stimulating electrodes, working electrodes, reference electrodes, and ultrasound transducer, according to the atlas of Paxinos and Watson.[64] Specifically, the carbon-fiber working electrode was lowered into the NAc core (+1.3 mm anterior-posterior [AP], +2.0 mm medial-lateral [ML], −7.1 mm dorsal-ventral [DV]), and the bipolar stimulating electrode (Plastics One, Roanoke, VA, USA) was lowered to the VTA (−4.7 mm AP, +0.9 mm ML, −8.5 mm DV). The dorsoventral coordinate of the electrodes was adjusted for maximally stimulated release. A 3.0 mm wide hole was drilled through the skull for the transducer placement to sonicate the dmPFC (+3.6 mm AP, +0.6 mm ML). In the first anatomical control, the hole for the transducer was drilled at the primary somatosensory cortex (3.2 mm AP, +0.6 mm ML), and dopamine was measured in the NAc core. In the second and third anatomical controls, dopamine was measured at the Caudate-Putamen (1.3 mm AP, 2.0 mm ML, −4.5 mm DV) and NAc shell (1.3 mm AP, 1.0 mm ML, −6.5 mm DV) respectively, while LIFU was applied to the PLC. An Ag/AgCl wire reference electrode was inserted on the contralateral side of the brain. To electrically stimulate dopamine, a constant biphasic current stimulus at +300 μA, 2 ms, 24 pulses was delivered to the VTA by a bipolar stimulating electrode (Plastics One, Inc., Roanoke, VA, USA). Dopamine was detected using FSCV, stimulations were delivered every 5 minutes, and dopamine release was measured at the NAc core (or control region) for 2.5 hours.

Ultrasound Characterization

A 10 MHz miniature-case immersion transducer (XMS-310-B, Olympus-ims, Waltham, MA) with a 2 mm element diameter and 6 mm focal length was used. Ultrasonic waveforms were generated

using a two-channel, 30 MHz Dual Channel Function/Arbitrary Waveform Generator (4054B; BK Precision, Yorba Linda, CA, USA) coupled with an amplifier (E&I 230L; Electronics and Innovation, Rochester NY, USA) and visualized using a 200MHz 4 Channel 2GS/s Oscilloscope (TDS2024C; Tektronix, Beaverton, OR, USA). Before use, the acoustic pressure field was quantified in an acoustic test tank filled with de-ionized, degassed, and filtered water (Ultrasonic Measurement System V3 (UMS3) Precision Acoustics Ltd Dorchester, UK) with a calibrated hydrophone (HNR-0500, Onda Corp., CA, USA). Throughout this study, we used pulsing parameters shown previously to induce local suppression of neuronal activity in different human brain areas.[19,50,51] We used 13 W/cm^2 as the baseline intensity for this study and examined the effects of doubling and halving this intensity.

Ultrasound Heating Modelling

Due to the high fundamental frequency used (10 MHz), there is the potential for ultrasound to create unwanted heating. To predict heating in tissue, we simulated heat transfer using Pennes bioheat equation: $\rho c\frac{\partial T}{\partial t} = \nabla^2 T + Q$ where T = temperature, ρ = density of the tissue, c = specific heat capacity of the tissue, k = thermal conductivity of the tissue and Q = heat source term (ultrasound). We ran a one-dimensional model assuming constant properties for uniform brain tissue temperature distribution and solved the equation using a finite difference method. Temperature rise was modeled using the exact parameters tested, including 2 minutes of 10 MHz ultrasound at three different intensities (6.5 W/cm^2, 13 W/cm^{2,} and 26 W/cm^2), using a 500-millisecond pulse at an inter-stimulus interval of 5 seconds.

Staining and *imaging* for tissue damage

After the dopamine measurements, rats (n=2) from the no-LIFU, 6.5 W/cm^2, 13 W/cm^{2,} and 26 W/cm^2 LIFU groups were perfused with PBS, followed by 4% paraformaldehyde. Brains were then collected and fixed in 4% PFA for 24 hours. 1 mm thick sections of the PLC and the NAc core were then taken using a brain matrix and dehydrated in 70% ethanol for sectioning. After being

embedded into paraffin at 58−60°C, the tissue specimen was sliced using an automatic microtome and then stained using Hematoxylin and eosin (H&E) at the University of Virginia histology core. The prepared histological sections were observed with an optical microscope (ZEISS Axio Examiner 2), and the images were analyzed using the Image J nuclei counter plug-in.

Statistics

All statistical analyses were performed in GraphPad Prism v. 10.0 (GraphPad Software, La Jolla, CA). Statistical p values were significant at a 95% confidence ($p < 0.05$). Values on plots are reported as the mean ± standard error of the mean (SEM), with n representing the number of brain slices. One-way ANOVA and Mixed-model effect analysis were also computed to examine the effect of LIFU sonication on data from different experimental time points.

References

1. Chinta, S. J. & Andersen, J. K. Dopaminergic neurons. *Int. J. Biochem. Cell Biol.* **37**, 942–946 (2005).
2. Kienast, T. & Heinz, A. Dopamine and the Diseased Brain. *CNS Neurol. Disord. - Drug Targets- CNS Neurol. Disord.* **5**, 109–131 (2006).
3. Grace, A. A. The tonic/phasic model of dopamine system regulation and its implications for understanding alcohol and psychostimulant craving. *Addiction* **95**, 119–128 (2000).
4. Bahi, A. & Dreyer, J. L. Dopamine transporter (DAT) knockdown in the nucleus accumbens improves anxiety- and depression-related behaviors in adult mice. *Behav. Brain Res.* **359**, 104–115 (2019).
5. Bressan, R. A. & Crippa, J. A. The role of dopamine in reward and pleasure behaviour – review of data from preclinical research. *Acta Psychiatr. Scand.* **111**, 14–21 (2005).
6. Blum, K. *et al.* Dopamine in the Brain: Hypothesizing Surfeit or Deficit Links to Reward and Addiction. *J. Reward Defic. Syndr.* **1**, 95–104 (2015).
7. Cooper, S., Robison, A. J. & Mazei-Robison, M. S. Reward Circuitry in Addiction. *Neurotherapeutics* **14**, 687–697 (2017).

8. Vialou, V. *et al.* Prefrontal Cortical Circuit for Depression- and Anxiety-Related Behaviors Mediated by Cholecystokinin: Role of ΔFosB. *J. Neurosci.* **34**, 3878–3887 (2014).
9. McGlinchey, E. M., James, M. H., Mahler, S. V., Pantazis, C. & Aston-Jones, G. Prelimbic to Accumbens Core Pathway Is Recruited in a Dopamine-Dependent Manner to Drive Cued Reinstatement of Cocaine Seeking. *J. Neurosci. Off. J. Soc. Neurosci.* **36**, 8700–8711 (2016).
10. Robinson, D. L., Zitzman, D. L. & Williams, S. K. Mesolimbic dopamine transients in motivated behaviors: Focus on maternal behavior. *Front. Psychiatry* **2**, 23 (2011).
11. Spagnolo, P. A. & Goldman, D. Neuromodulation interventions for addictive disorders: challenges, promise, and roadmap for future research. *Brain J. Neurol.* **140**, 1183–1203 (2017).
12. Siddiqi, S. H. *et al.* Brain stimulation and brain lesions converge on common causal circuits in neuropsychiatric disease. *Nat. Hum. Behav.* **5**, 1707–1716 (2021).
13. Figee, M. *et al.* Deep Brain Stimulation for Depression. *Neurother. J. Am. Soc. Exp. Neurother.* **19**, 1229–1245 (2022).
14. Berke, J. D. & Hyman, S. E. Addiction, dopamine, and the molecular mechanisms of memory. *Neuron* **25**, 515–532 (2000).
15. Bestmann, S. & Walsh, V. Transcranial electrical stimulation. *Curr. Biol.* **27**, R1258–R1262 (2017).
16. Sparing, R. & Mottaghy, F. M. Noninvasive brain stimulation with transcranial magnetic or direct current stimulation (TMS/tDCS)—From insights into human memory to therapy of its dysfunction. *Methods* **44**, 329–337 (2008).
17. Deng, Z.-D., Lisanby, S. H. & Peterchev, A. V. Electric field depth–focality tradeoff in transcranial magnetic stimulation: simulation comparison of 50 coil designs. *Brain Stimulat.* **6**, 1–13 (2013).
18. Darmani, G. *et al.* Non-invasive transcranial ultrasound stimulation for neuromodulation. *Clin. Neurophysiol.* **135**, 51–73 (2022).

19. Legon, W. *et al.* Transcranial focused ultrasound modulates the activity of primary somatosensory cortex in humans. *Nat. Neurosci.* **17**, 322–329 (2014).

20. Xu, T. *et al.* Ultrasonic stimulation of the brain to enhance the release of dopamine – A potential novel treatment for Parkinson's disease. *Ultrason. Sonochem.* **63**, 104955 (2020).

21. Min, B.-K. *et al.* Focused ultrasound modulates the level of cortical neurotransmitters: Potential as a new functional brain mapping technique. *Int. J. Imaging Syst. Technol.* **21**, 232–240 (2011).

22. Robinson, D. L., Venton, B. J., Heien, M. L. A. V. & Wightman, R. M. Detecting subsecond dopamine release with fast-scan cyclic voltammetry in vivo. *Clin. Chem.* **49**, 1763–1773 (2003).

23. Venton, B. J. & Cao, Q. Fundamentals of fast-scan cyclic voltammetry for dopamine detection. *Analyst* **145**, 1158–1168 (2020).

24. Venton, B. J. *et al.* Real-time decoding of dopamine concentration changes in the caudate-putamen during tonic and phasic firing. *J. Neurochem.* **87**, 1284–1295 (2003).

25. Kiyatkin, E. A. Brain temperature and its role in physiology and pathophysiology: Lessons from 20 years of thermorecording. *Temp. Austin Tex* **6**, 271–333 (2019).

26. Del Arco, A. & Mora, F. Glutamate-dopamine in vivo interaction in the prefrontal cortex modulates the release of dopamine and acetylcholine in the nucleus accumbens of the awake rat. *J. Neural Transm. Vienna Austria 1996* **112**, 97–109 (2005).

27. Guo, H. *et al.* Ultrasound Produces Extensive Brain Activation via a Cochlear Pathway. *Neuron* **98**, 1020-1030.e4 (2018).

28. Benarroch, E. E. Involvement of the nucleus accumbens and dopamine system in chronic pain. *Neurology* **87**, 1720–1726 (2016).

29. Ding, D. C. D., Gabbott, P. L. A. & Totterdell, S. Differences in the laminar origin of projections from the medial prefrontal cortex to the nucleus accumbens shell and core regions in the rat. *Brain Res.* **917**, 81–89 (2001).

30. Clark, J. J. *et al.* Chronic microsensors for longitudinal, subsecond dopamine detection in behaving animals. *Nat. Methods* **7**, 126–9 (2010).

31. Gao, M. *et al.* Functional Coupling between the Prefrontal Cortex and Dopamine Neurons in the Ventral Tegmental Area. *J. Neurosci.* **27**, 5414–5421 (2007).

32. Fields, H. L., Hjelmstad, G. O., Margolis, E. B. & Nicola, S. M. Ventral Tegmental Area Neurons in Learned Appetitive Behavior and Positive Reinforcement. *Annu. Rev. Neurosci.* **30**, 289–316 (2007).

33. Roitman, M. F., Wheeler, R. A., Wightman, R. M. & Carelli, R. M. Real-time chemical responses in the nucleus accumbens differentiate rewarding and aversive stimuli. *Nat. Neurosci.* **11**, 1376–1377 (2008).

34. Buck, S. A., Torregrossa, M. M., Logan, R. W. & Freyberg, Z. Roles of dopamine and glutamate co-release in the nucleus accumbens in mediating the actions of drugs of abuse. *FEBS J.* **288**, 1462–1474 (2021).

35. Bauter, M. R., Brockel, B. J., Pankevich, D. E., Virgolini, M. B. & Cory-Slechta, D. A. Glutamate and dopamine in nucleus accumbens core and shell: sequence learning versus performance. *Neurotoxicology* **24**, 227–243 (2003).

36. Huffman, M. L. & Venton, B. J. Carbon-fiber microelectrodes for in vivo applications. *The Analyst* **134**, 18–24 (2009).

37. Rafi, H. & Zestos, A. G. Review—Recent Advances in FSCV Detection of Neurochemicals via Waveform and Carbon Microelectrode Modification. *J. Electrochem. Soc.* **168**, 057520 (2021).

38. Banerjee, S., McCracken, S., Hossain, M. F. & Slaughter, G. Electrochemical Detection of Neurotransmitters. *Biosensors* **10**, 101 (2020).

39. Ganesana, M., Trikantzopoulos, E., Maniar, Y., Lee, S. T. & Venton, B. J. Development of a novel micro biosensor for in vivo monitoring of glutamate release in the brain. *Biosens. Bioelectron.* **130**, 103–109 (2019).

40. Hamilton, M. E., Mele, A. & Pert, A. Striatal extracellular dopamine in conscious vs. anesthetized rats: effects of chloral hydrate anesthetic on responses to drugs of different classes. *Brain Res.* **597**, 1–7 (1992).

41. Warenycia, M. W. & McKenzie, G. M. Excitation of striatal neurons by dexamphetamine is not abolished by either chloral hydrate or urethane anaesthesia. *Neuropharmacology* **27**, 1309–1312 (1988).

42. Hernández, G. & Shizgal, P. Dynamic changes in dopamine tone during self-stimulation of the ventral tegmental area in rats. *Behav. Brain Res.* **198**, 91–97 (2009).

43. Hernandez, G. *et al.* Prolonged rewarding stimulation of the rat medial forebrain bundle: Neurochemical and behavioral consequences. *Behav. Neurosci.* **120**, 888–904 (2006).

44. Mohammadjavadi, M. *et al.* Transcranial ultrasound neuromodulation of the thalamic visual pathway in a large animal model and the dose-response relationship with MR-ARFI. *Sci. Rep.* **12**, 19588 (2022).

45. Darrow, D. P., O'Brien, P., Richner, T., Netoff, T. I. & Ebbini, E. S. A thermal mechanism underlies tFUS neuromodulation. *Brain Stimulat.* **13**, 327–328 (2020).

46. Yoo, S.-S. *et al.* Focused ultrasound modulates region-specific brain activity. *NeuroImage* **56**, 1267–1275 (2011).

47. O'Brien, W. D. *et al.* The Risk of Exposure to Diagnostic Ultrasound in Postnatal Subjects: Thermal Effects. *J. Ultrasound Med.* **27**, 517–535 (2008).

48. Kubanek, J., Shukla, P., Das, A., Baccus, S. A. & Goodman, M. B. Ultrasound Elicits Behavioral Responses through Mechanical Effects on Neurons and Ion Channels in a Simple Nervous System. *J. Neurosci.* **38**, 3081–3091 (2018).

49. Tyler, W. J. The mechanobiology of brain function. *Nat. Rev. Neurosci.* **13**, 867–878 (2012).

50. Legon, W., Bansal, P., Tyshynsky, R., Ai, L. & Mueller, J. K. Transcranial focused ultrasound neuromodulation of the human primary motor cortex. *Sci. Rep.* **8**, 10007 (2018).

51. Legon, W., Ai, L., Bansal, P. & Mueller, J. K. Neuromodulation with single-element transcranial focused ultrasound in human thalamus. *Hum. Brain Mapp.* **39**, 1995–2006 (2018).

52. King, R. L., Brown, J. R., Newsome, W. T. & Pauly, K. B. Effective Parameters for Ultrasound-Induced In Vivo Neurostimulation. *Ultrasound Med. Biol.* **39**, 312–331 (2013).

53. Hoffman, B. U. *et al.* Focused ultrasound excites action potentials in mammalian peripheral neurons in part through the mechanically gated ion channel PIEZO2. *Proc. Natl. Acad. Sci.* **119**, e2115821119 (2022).

54. Drion, G., O'Leary, T. & Marder, E. Ion channel degeneracy enables robust and tunable neuronal firing rates. *Proc. Natl. Acad. Sci.* **112**, (2015).

55. Yoo, S., Mittelstein, D. R., Hurt, R. C., Lacroix, J. & Shapiro, M. G. Focused ultrasound excites cortical neurons via mechanosensitive calcium accumulation and ion channel amplification. *Nat. Commun.* **13**, 493 (2022).

56. Ranade, S. S., Syeda, R. & Patapoutian, A. Mechanically Activated Ion Channels. *Neuron* **87**, 1162–1179 (2015).

57. Sorum, B., Rietmeijer, R. A., Gopakumar, K., Adesnik, H. & Brohawn, S. G. Ultrasound activates mechanosensitive TRAAK K+ channels through the lipid membrane. *Proc. Natl. Acad. Sci.* **118**, e2006980118 (2021).

58. Yaakub, S. N. *et al.* Transcranial focused ultrasound-mediated neurochemical and functional connectivity changes in deep cortical regions in humans. *Nat. Commun.* **14**, 5318 (2023).

59. Mahoney, J. J. *et al.* Low-intensity focused ultrasound targeting the nucleus accumbens as a potential treatment for substance use disorder: safety and feasibility clinical trial. *Front. Psychiatry* **14**, (2023).

60. Whitfield, T. W., Shi, X., Sun, W.-L. & McGinty, J. F. The Suppressive Effect of an Intra-Prefrontal Cortical Infusion of BDNF on Cocaine-Seeking Is Trk Receptor and Extracellular Signal-Regulated Protein Kinase Mitogen-Activated Protein Kinase Dependent. *J. Neurosci.* **31**, 834–842 (2011).

61. Bakhti-Suroosh, A., Towers, E. B. & Lynch, W. J. A buprenorphine-validated rat model of opioid use disorder optimized to study sex differences in vulnerability to relapse. *Psychopharmacology (Berl.)* **238**, 1029–1046 (2021).

62. Strohman, A., Payne, B., In, A., Stebbins, K. & Legon, W. Low-intensity focused ultrasound to the human dorsal anterior cingulate attenuates acute pain perception and autonomic responses. *J. Neurosci. Off. J. Soc. Neurosci.* e1011232023 (2024) doi:10.1523/JNEUROSCI.1011-23.2023.

63. Legon, W., Strohman, A., In, A., Stebbins, K. & Payne, B. Non-invasive neuromodulation of sub-regions of the human insula differentially affect pain processing and heart-rate variability. *BioRxiv Prepr. Serv. Biol.* 2023.05.05.539593 (2023) doi:10.1101/2023.05.05.539593.

64. Paxinos, G. & Watson, C. *The Rat Brain in Stereotaxic Coordinates*. (Elsevier Academic Press, Amsterdam-Boston, 2007).